

Primary stage of Fe-Cr-C alloy oxidation at 1100°C

M. Hajduga*, D. Jędrzejczyk

Technical University of Bielsko-Biała,
ul. Willowa 2, 43-309 Bielsko-Biała, Poland

* Corresponding author: E-mail address: mhajduga@ath.bielsko.pl

Received 10.09.2010; published in revised form 01.11.2010

Manufacturing and processing

ABSTRACT

Purpose: To study the primary oxidation stage of Fe-Cr-C steels in more detail, to correlate the oxidation kinetics with O₂ absorption, with CO₂ evolution and with the morphology of the scale layers formed during the course of oxidation.

Design/methodology/approach: Analysis of oxidation kinetic of Fe-Cr-C alloys containing 13 % Cr and carbon ranging from 0.15 to 1.63% at 1100°C for 3hr was carried out using a SETA-RAM-1000 thermobalance-chromatograph. Three specimen geometries were used: cylindrical specimens, bar-like samples, wire-like samples. As a results the weight gain relations, measured rates of carbon loss, rates of oxygen absorption and morphology of the oxide scales was analysed.

Findings: The oxidation rate increased with increasing carbon content in the alloys. The measured time variation of CO₂ evolution showed that, during the first period of oxidation (0-40 min), a compact surface layer of FeO formed, which prohibited the free transfer of CO₃ into the streaming oxidation atmosphere. The measurable CO₂ evolution started between 40 and 50 min, and the most rapid evolution occurred in the interval t = 60-90 min of oxidation. This effect corresponds well to scale-layer damage and to the maximum O₂ absorption.

Research limitations/implications: Results enable to interpret the primary stage of the oxidation of Fe-Cr-C alloys and to discuss the relations between the cation diffusivities in the individual oxide sublayers, i.e., in wustite, magnetite, and hematite.

Originality/value: More detailed description of the primary oxidation stage of Fe-Cr-C steels.

Keywords: Oxidation; Iron-chromium-carbon; Decarburization; Scales morphology; Cation diffusion

Reference to this paper should be given in the following way:

M. Hajduga, D. Jędrzejczyk, Primary stage of Fe-Cr-C alloy oxidation at 1100°C, Journal of Achievements in Materials and Manufacturing Engineering 43/1 (2010) 403-408.

1. Introduction

A look at the contemporary published papers concerning the oxidation of Fe-Cr-C alloys [1] shows that the volume of these contributions is not very large. The predominating number of the published works deal with Fe-C [2-4] or with Fe-Cr alloys [5-9]. In many experiments carried out with these materials, the oxidation temperatures were below 1000°C, and the oxidation periods

were on the order of tens to hundreds of hours. In these long-term experiments the primary stages of oxidation are omitted, as a rule, and the measured values are extrapolated to the $t = 0$ point by the standard parabolic dependence.

Oxidation of industrial materials was confined mainly to the commercial superalloys [10] for exposures in still air up to 1150°C for periods up to 10⁴ hr. This group of materials includes the alloys of the sort Fe-13%Cr-X%C with $X = 0.15-1.63$. As far as we know, the oxidation of these materials has not yet been

Table 1.
Chemical Composition of the Oxidized Steels (wt.%)

Steel mark	Element [wt.]						
	C	Mn	Si	P	S	Cr	Ni
NC10	1.63	0.34	0.44	0.023	0.023	12.77	Traces
D	0.97	0.24	0.10	0.026	0.030	12.67	0.09
E	0.50	0.20	0.10	0.026	0.019	12.52	0.10
3H13	0.30	0.39	0.29	0.027	0.017	12.90	0.26
1H13	0.15	0.40	0.26	0.030	0.029	13.22	0.32

Table 2.
Parameters of the Linear Weigh Gain versus Time for Oxidation of Various Steels

Steel mark	Carbon content, wt. %	$(w_2/q)_0$, mg·cm ⁻²	10^4k , mg·cm ⁻² ·sec ⁻¹	10^2v_c , cm ³ ·sec ⁻¹
NC10	1.63	0.679±0.007	2.485±0.025	46.17±0.37
D	0.97	0.440±0.023	2.546±0.011	28.25±1.22
E	0.50	0.684±0.019	2.493±0.030	16.85±1.23
3H13	0.30	0.173±0.017	0.566±0.023	3.20±0.73
1H13	0.15	0.559±0.011	0.454±0.015	6.63±1.03

*See Eq. (1) and Fig. 1. Sample surface $q = 7.85\text{cm}^2$; v_c gives the effective calculated flow rate [Eq.(4)]

studied. The published results [5] show that the carbon content decreased the oxidation rate of Fe-C steels with respect to pure Fe. By contrast, the higher content of C increased the oxidation rate of Fe-C steels [3].

Based on the facts mentioned above, it was decided to study the primary oxidation stage of Fe-Cr-C steels in more detail, to correlate the oxidation kinetics with O_2 ; absorption, with CO_2 evolution and with the morphology of the scale layers formed during the course of oxidation.

2. Experimental

The chemical composition of the steels is given in Table 1. Three specimen geometries were used: 1 - cylindrical specimens having dimensions $\phi = 10$ mm and $L = 20$ mm were used in the studies of oxidation kinetics, 2 - bar-like samples with $\phi = 50$ mm and $L = 2000$ mm were used in the production and preparation of the separated oxide scales [13]; 3- wire-like samples with $\phi = 3$ mm and $L = 30$ mm were used for the common metallographic studies of the surface oxide layers.

The specimens of type 1 were machined from hot-rolled cylindrical bars, which had the dimensions $\phi = 50$ mm and $L = 3000$ mm. The orientation of the specimen axis, with respect to the rolling direction, was random. A 0.3mm suspension hole was drilled near the middle of one end of the sample. The machined specimens were then abraded with abrasive papers through 1000 grit and polished by means of metallographic paste, carefully washed in distilled water and dried in hot air.

The kinetics measurements were carried out using a SETARAM-1000 thermobalance coupled to a recorder that had a sensitivity of ± 2.2 mg at the 12.3-g load. The specimens were suspended on a platinum wire in the reaction tube of the thermobalance. After the interior space of the balance had been evacuated to 13.3 MPa, the oxidation atmosphere was flowed

through it with a low overpressure and an effective flow rate in the range of 6×10^{-2} up to $46 \times 10^{-2} \text{cm}^2 \cdot \text{sec}^{-1}$ (Table 2.). Small variations in the flow rate were caused by fluctuations of the overpressure and, probably, by some fluctuations of the composition of the oxidation atmosphere. The nominal atmosphere composition was, in volume %: 4.8 O_2 , 1.2 N_2 , and 94 He with the standard technical gas purity.

Simultaneously with the oxidation atmosphere flow the thermoregulator was started, which increased the specimen temperature up to 1100°C during a time period of 36-37 min at a rate of 30°C/min. The oxidation temperature was kept constant within $\pm 2^\circ\text{C}$. The rate of CO_2 evolved during the oxidation and the rate of unreacted O_2 were measured in vol.% by passing the exhaust gases from the reaction tube through a chromatograph. After 3 hr of oxidation the specimen was removed from the balance, put into a desiccator and preserved for subsequent metallographic investigations. Three specimens of each alloy (Table 1.) were used in the oxidation experiments.

3. Oxidation kinetics

The measured weight gain-time curves for the individual Fe-Cr-C alloys are shown in Fig. 1. It can be seen that a measurable weigh gain started in the time interval of 3-10 min., i.e., at temperatures of 100-300°C.

The first period of the oxidation (up to about 45 min.) is characterized by a high rate of weight gain, especially in the cases of the steels with higher carbon content (Fig. 2). After reaching steady state, at about 40-50 min - the second period - the samples oxidized by a linear law [13]:

$$w_2(t)/q = (w_2/q)_0 + kt \quad (1)$$

where $a = (785 \pm 2) \text{mm}^2$ is the total sample surface, k is the linear rate constant, and the subscript 2 denotes the second period of the

primary stage of oxidation. The parameters $(w_2/q)_0$ and k , evaluated from the experimental data, are presented in Table 2. The rate constant k is a step like function of the carbon concentration N_C . It takes the value of about $0.5 \times 10^{-4} \text{ mg}\cdot\text{cm}^{-2}\cdot\text{sec}^{-1}$ at the low carbon content (0.15 and 0.30% C) and the value $k \approx 2.5 \times 10^{-4}$ at the concentrations $\geq 0.50\%$ C. These results are in good agreement with those published by Trafford and Whittle [7], who give a linear weight gain-time curve with $k = 1.74 \times 10^{-5} \text{ mg cm}^{-2}\cdot\text{sec}^{-1}$ for the alloy Fe-13%Cr and $N_C \rightarrow 0$ oxidized at $900^\circ\text{C}/3 \text{ hr}$ in slowly flowing oxygen at 0.101 MPa.

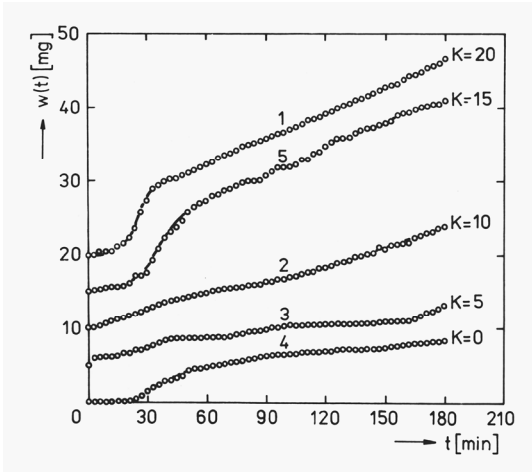


Fig. 1. Weight gain-versus-time curves for Fe-Cr-C steels oxidized at 1100°C ; (0000) experimental values; K, redundant additive constant, 1-NC10; 2-E, 3-3H13, 4-1H13, 5-D

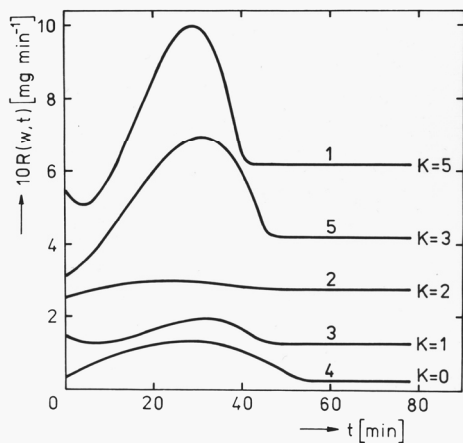


Fig. 2. Calculated rates of the weight gain in the first period (0-45min) of oxidation, K - redundant additive constant. 1-NC10; 2-E, 3-3H13, 4-1H13, 5-D

The first period of the primary stage of oxidation is characterized by a relatively high rate of the weight gain (see Figs. 1 and 2). Trying to find the appropriate rate characteristics corresponding to

the k value from Table 2, we expressed the weight gains in the first period by the form of the polynomial function:

$$w_i(t) = \sum_{i=0}^4 a_i t^i \quad (2)$$

The individual parameters a_i evaluated from the experimental data are presented in Table 3. No systematic trends, corresponding to the concentration variation of the constant k (Table 2.), can be claimed for these parameters. However, on the basis of the parameters a_i it is easy to obtain the weight-gain rates $R(w_i) = dw_i/dt$ shown in Fig. 2.

The calculated values $R(w_i)$ increase in the time interval $t = 0$ up to about 30 min.; after reaching the maximum, they decrease to the k values, which are the characteristics of the linear law (1) for the second stage of oxidation.

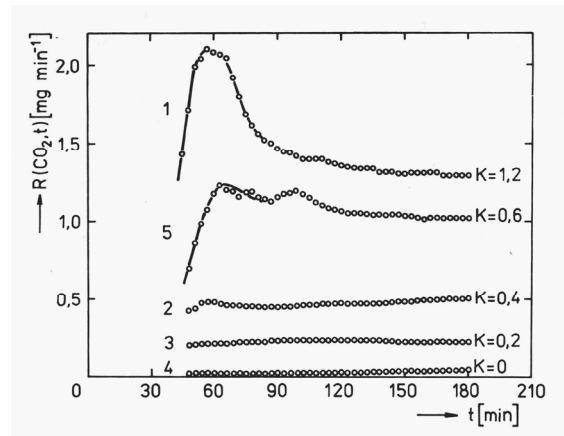


Fig. 3. Measured rates of carbon loss; (0000) experimental values, K redundant additive constant. 1-NC10; 2-E, 3-3H13, 4-1H13, 5-D

The oxidation and decarburization kinetics were measured by simultaneously analyzing the exhaust gases from the thermobalance for CO_2 and O_2 . The measured rates of carbon loss $R(\text{CO}_2)$ and oxygen absorption $R(\text{O}_2)$ are shown as functions of time in Figs. 3 and 4. The total amounts of CO_2 evolved and O_2 absorbed are given as integrals

$$I(X_i, t) = \int_0^t R(X_i, \tau) d\tau \quad (3)$$

in Figs. 5 and 6; X_i stands for CO_2 , or O_2 .

It is shown in Figs. 3 and 4 that the measurable loss of CO_2 starts at $t \approx 40$ min, i.e., approximately at the time at which thermal equilibrium in the balance is reached, and that the time behavior of $R(\text{CO}_2, t)$ is similar to that of $R(\text{O}_2, t)$. The maximum rate of CO_2 loss, corresponding to the maximum O_2 absorption, occurs in steels with higher C content at about $t = 60$ min. This effect can not be claimed for 1H13 and 3H13 steels, in which the C content is lower and in which the measurements of $R(\text{CO}_2, t)$ are more difficult.

Table 3. Parameters or the Polynomial Functions (2) Describing Weight Gain in the First Period, O-t₁ or the Primary Stage of Oxidation

Steel mark	t ₁ , min	a ₀ ×10 ² , mg	a ₁ ×10 ² , mg·min ⁻¹	a ₂ ×10 ³ , mg·min ⁻²	a ₃ ×10 ⁴ , mg·min ⁻³	a ₄ ×10 ⁶ , mg·min ⁻⁴
NC10	45	1.1433	5.5201	11.4930	10.5690	-15.9720
D	48	5.5192	1.1834	3.6755	3.9976	-4.4884
E	48	0.00*	5.3233	2.0916	-0.3724	0.1769
3H13	48	-4.4355	4.1241	-3.0152	1.8043	-2.2810
1H13	57	-4,2683	3.3227	3.0348	-0.1985	-0.2849

* With this value, the optimum fit was achieved

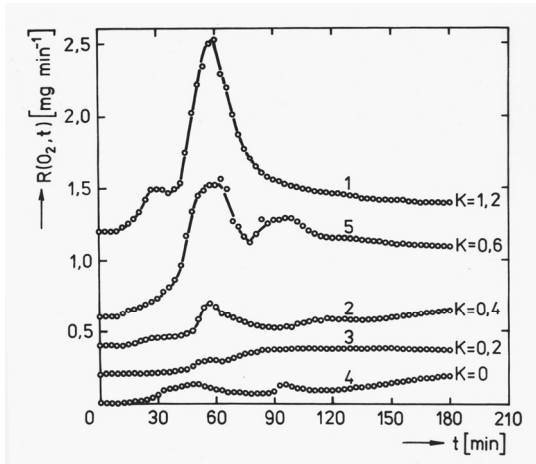


Fig. 4. Measured rates of oxygen absorption. (0000) experimental values, K - redundant additive constant, 1-NC10; 2-E, 3-3H13, 4-1H13, 5-D

Measurable rates of R(O₂, t) (Fig. 4) appear at about t = 12 min. Afterward, they increase with time and reach, in accordance with R(CO₂, t) curves, a maximum at the time t ≈ 60 min. It is worth noting that the time variation of R(O₂, t) for NC10 steel (1.63% C) revealed a local maximum at t = 30 min. This corresponds well to the maximum of the weight gain rate (Fig. 2) occurring at the time at which the nominal oxidation temperature is reached.

The values of w(t), R(O₂, t), R(CO₂, t) yield an interesting possibility to calculate the effective flow rate v_c of the oxidizing atmosphere. The basis for these calculations is the law of conservation. Since the experimental values R(O₂, t) and R(CO₂, t) were measured in vol.% of the flowing oxidation atmosphere, the law of conservation takes, in this particular case, the form:

$$w(t) = v_c \left[\int_0^t \frac{R(O_2, t)}{100} s(O_2) dt - \int_0^t \frac{R(CO_2, t)}{100} s(CO_2) dt \right] \quad (4)$$

where s(O₂) and s(CO₂) are the densities given (in mg · cm⁻³). Inserting the experimental values w(t), R(O₂, t), R(CO₂, t) measured at t = (30 min) × n (n is an integer) and the densities into Eq. (4), we obtain the values v_c, the average of which are presented in Table 2.

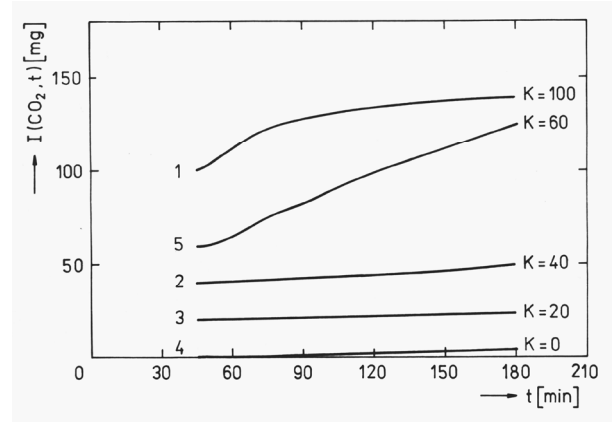


Fig. 5. The total calculated amount of CO₂ evolution Eq. 3, as a function of time of oxidation; K - redundant additive constant, 1-NC10; 2-E, 3-3H13, 4-1H13, 5-D.

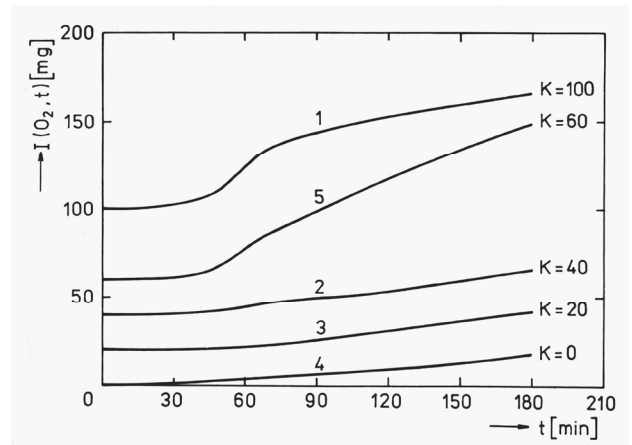


Fig. 6. Total calculated amount or O₂ absorbed Eq. (3), as a function of time, K - redundant additive constant, 1-NC10; 2-E, 3-3H13, 4-1H13, 5-D

We may remark that the nominal experimental values v_{exp} used in the individual measurements were situated in the interval 4 to 50 cm³sec⁻¹ and that the data plotted in Figs. 3-6 (in

milligrams) were calculated in the way indicated in Eq. (4) from the experimental values measured in vol.%.

4. Morphology of the oxide scales

Figures 7 and 8 show the total oxide layers formed during oxidation for 3 hr at 1100°C on the NC10 (Table 1.) steel surface. The scales shown in Fig. 7 were formed on a rod like sample [12] type (2), and those in Fig. 8 on a wire-like sample, type (3). Debye-Scherrer X-ray diffraction patterns of the scales [15] indicated that all three oxides of iron (FeO, Fe₃O₄, and Fe₂O₃) were present. In addition, the small amounts of chromite and of Cr₇C carbide were detected. The outer scale layer consisted of hematite, followed by magnetite and the innermost layer being wustite. It is clear in Fig. 7 that these phases form three well-defined parallel-sided layers, with magnetite and hematite accounting (Fig. 8) for approximately 40% of the total scale thickness. The individual scale layers are highly porous and differ from one another by their internal structure. The wustite layer may be denoted as a laminar one, the magnetite and hematite layers are more fine grained, (Fig. 9). All three layers contain a large number of cavities and cracks. Some of them reach up to the FeO/steel interface (Fig. 8).

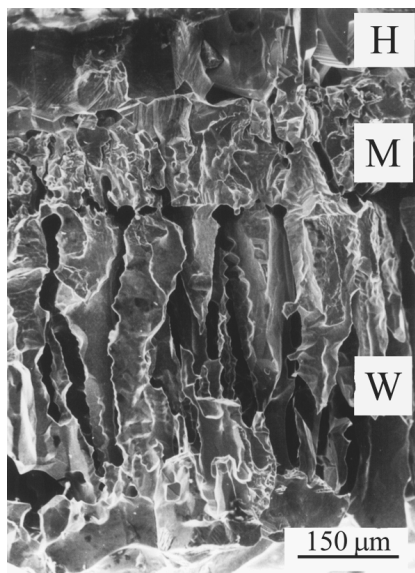


Fig. 7. SEM photomicrograph of the scale fracture plane, oxidized in air at 1100°C/3 hr. Sample (2). $\phi=50$ mm, $L=200$ mm, steel NC10. H, hematite; M, magnetite; W, wustite

5. Discussion and summary

The measurable oxidation of Fe-13Cr-C steels starts under the conditions applied in the present work at the very beginning of oxidation (Fig. 1). In all the investigated steels, the primary stage of oxidation occurs in two periods. The first one, from 0 up to

about 45 min, coincides in a greater part with the time interval (0-30 min) of the temperature rise of the samples.

The weight gain rate in the first period may be well described (Table 3.) by a parabola. It reaches its maximum at about 30 min, further on it decreases and starts to be a constant at about 45 min. This time it represents the beginning of the second period characterized by linear variation of the weight gain $w_2(t)$ with time. This indicates that the factor controlling the oxidation rate $dw_2(t)/dt$ is the chemical reaction occurring at the FeO/steel interface [13].

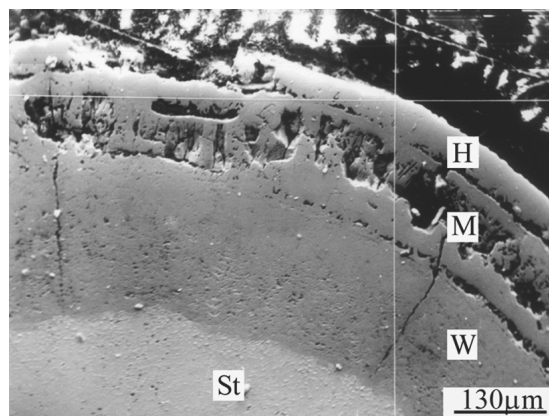


Fig. 8. Part of the cross section of NC10 steel wire, oxidized in air at 1100°C/3 hr, sample (3), $\phi=3$ mm, $L=30$ mm, H, hematite; M, magnetite; W, wustite; St steel

Furthermore, the linear weight gain in the second period $w_2(t)$ correlates well with the morphology of the oxide scales characterized by extended porosity (Fig. 7), by cracks (Fig. 8), and by a high occurrence of cavities (Fig. 8). Because of these cracks and cavities, the oxidation atmosphere is in continuous contact with the metallic surface [12] and the evolved CO₂ leaks out from the FeO-metal interface. The weigh-gain rate (Table 2.) depends on carbon content in the steel. Its value is about five times lower at concentrations of 0.15 and 0.30% C than the weight-gain rate at $N_c \geq 0.050\%$ C. This is analogous to the results dealing with the oxidation of Fe-C alloys at 850°C [5]. The parabolic rate constants given for 0.1% C and for 0.4% C have the values $1.2 \times 10^{-3} \text{ mg}^2/\text{cm}^2 \cdot \text{sec}$ and $16 \times 10^{-3} \text{ mg}^2/\text{cm}^2 \cdot \text{sec}$. [5]. Moreover, our results may be well compared with those published by Trafford and Whittle [7], who have investigated the oxidation of Fe-13%Cr alloys (C content is not given) at 900 °C in slow-flowing oxygen, 0.1013 MPa. Trafford and Whittle [7] stated that the weight gain starts to be linear at a time of about 720 min which is account 15 times more than the value given in the present paper (Table 3.). This difference may be caused, primarily, by the difference in oxidation temperatures, 850 and 1100°C. The parameters of the linear equation (I) evaluated from the data [7] have the values $(w/q)_0 = 3.8 \text{ mg} \cdot \text{cm}^{-2}$ and $10^4 k = 0.174 \text{ mg} \cdot \text{cm}^{-2} \cdot \text{sec}^{-1}$. These parameters, especially the rate constant k , correspond well to the data given in Table 2 for 0.15% C, even if their experimental conditions [8] and ours were rather different.

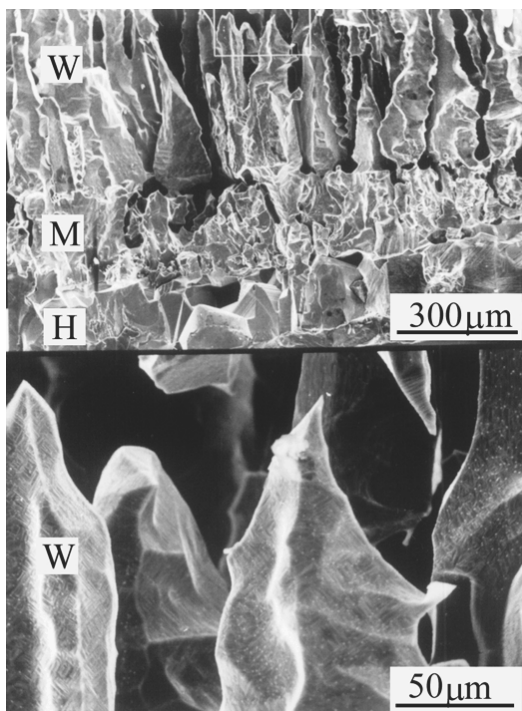


Fig. 9. SEM photomicrograph of the scale fracture plane, oxidized in air at 1100°C/3hr, sample (2), $\phi=50\text{mm}$, $L=200\text{mm}$, steel NC10; a - total scale layer, b - detail of wustite sublayer.

The evolution of CO_2 (Fig. 3) begins at approximately 45 min. Its rate reaches a maximum at 60 min. Simultaneously with the start of CO_2 evolution the linear weight-gain begins to operate. This means that at this time O_2 penetrates freely to the FeO -steel interface again, and the reaction $\text{O}_2 + 2\text{Fe} = 2(\text{FeO})$ occurs.

The oxygen absorption (Fig. 4), measured as O_2 entering minus O_2 leaving the thermobalance, corresponds well with the results given in Fig. 3. The maximum in Fig. 4 at ≈ 60 min coincides with the maximum of CO_2 evolution rate (Fig. 3).

The total weight gain (Fig. 1), O_2 absorption (Fig. 6), and the total CO_2 evolved (Fig. 5) yield the possibility of calculating the flow rate of the oxidation atmosphere - Eq. (3) and (4). The calculated values v_c , presented in Table 3 are placed well in the interval $v_{\text{exp}} = 4.2$ to $50 \text{ cm}^3 \cdot \text{sec}^{-1}$ of the nominal experimental values.

The observed morphology of oxide scales (Figs. 7-9) enlightens, to a certain extent, the oxidation and decarburization behavior of Fe-Cr-C alloys. The cracks, numerous cavities in the scale layers and the developed porosity make the penetration of O_2 to the FeO_2 - steel interface possible. This ensures the linear weight gain, as well as the CO_2 evolution during the second period of the primary stage of oxidation. The highly porous structure of the scale layers, (Fig. 7) and of the wustite especially (Fig. 9) makes it possible to understand, at least qualitatively, the diffusion behavior in oxides. The higher porosity of wustite

suggests that $D_W^{\text{Fe}} \gg D_M^{\text{Fe}}$, and $D_W^{\text{Fe}} \gg D_H^{\text{Fe}}$, D_W^{Fe} , D_M^{Fe} , and D_H^{Fe} are the appropriate Fe diffusivities in the individual oxide sublayers. Using the diffusion characteristics we can remark that $D_W^{\text{Fe}} / D_M^{\text{Fe}} = 3.07 \times 10^5$ and $D_W^{\text{Fe}} / D_H^{\text{Fe}} = 6.42 \times 10^5$ at 1100°C. It may be concluded from these values and from the scales morphology that the bulk diffusion in wustite is expressively influenced by the surface diffusion in the pores and cavities. In indirect support of this notion, the ratio of the surface diffusivity [14] to the bulk diffusivity [15] in γFe has the value $(D_{\gamma\text{Fe}}^{\text{Fe}})_r / (D_{\gamma\text{Fe}}^{\text{Fe}})_b = 2.15 \times 10^7$ at $T = 1100^\circ\text{C}$.

References

- [1] A.U. Malik, High-temperature oxidation of transition metal carbide-dispersed iron-base alloys, *Oxidation of Metals* 24 (1985) 233-263.
- [2] J. Baud, A. Ferrier, J. Manenc, J. Benard, The oxidation and decarburizing of Fe-C alloys in air and the influence of relative humidity, *Oxidation of Metals* 9 (1975) 69
- [3] D. Caplan, C.I. Sproule, R.J. Hussey, M.J. Graham, Oxidation of Fe-C alloys at 500 °C, *Oxidation of Metals* 12/1 (1978) 67-82.
- [4] D. Caplan, G.I. Sproule, R.J. Hussey, M.J. Graham, Oxidation of Fe-C Alloys at 700 °C, *Oxidation of Metals* 13/3 (1979) 255-263.
- [5] A.U. Malik, D.P. Whittle, Oxidation of Fe-C alloys in the temperature range 600-850 °C *Oxidation of Metals*. 16/5-6 (1981) 339-353.
- [6] O.T. Goncel, D.P. Whittle, J. Stringer, The oxidation behavior of Fe-Cr alloys containing HfO_2 -dispersed phase, *Oxidation of Metals* 15/3-4 (1981) 287-295.
- [7] D.N.H. Trafford, D.P. Whittle, The salt-induced corrosion behavior of Fe-Cr alloys at elevated temperatures, *Corrosion Science* 20/4 (1980) 497-507.
- [8] Y. Ikeda, K. Nii, Microcrack generation and its healing in the oxide scale formed on Fe-Cr alloys, *Oxidation of Metals* 12/6 (1978) 487-502.
- [9] C.U Angerman, Long-term oxidation of superalloys, *Oxidation of Metals* 5/2 (1972) 149-167.
- [10] J. Manenc, G.Vagnard, Etude De L'oxydation D'alliages Fer-Carbone, *Corrosion Science* 9 (1969) 857-868.
- [11] J. Baud, J.P. Plumensi, J. Manenc, Influence de l'adherence de la calamine sur la concentration du carbone au voisinage de la surface des aciers. *Materials and Corrosion* 23/10 (1972) 866-880.
- [12] M. Hajduga, J. Kucera, Primary stage of Fe-Cr-C alloys oxidation at 1100 °C, *Oxidation of Metals* 29/1-2 (1988) 121-133.
- [13] K. Hauffe, Reaktionen in und an Festen Stoffen, Springer-Verlag, Berlin, 1955.
- [14] G. Neumann, G.M. Neumann, Surface Self-Diffusion of Metals, F. H. Wohlbier, ed. Solothurn, Switzerland, 1982.
- [15] J. Kucera, K. Stransky, Diffusion in iron, iron solid solution and steels, *Materials Science and Engineering* 52/1 (1982) 1-38.